Published in the Russian Federation
European Journal of Molecular Biotechnology
Has been issued since 2013.
ISSN: 2310-6255
E-ISSN: 2409-1332
Vol. 14, Is. 4, pp. 125-138, 2016

DOI: 10.13187/ejmb.2016.14.125
www.ejournal8.com

Comparative Modeling the Thermal Transfer in Tissues with Volume Pathological Focuses and Tissue Engineering Constructs: a Pilot Study

Valery V. Novochadov [a], Alexander A. Shiroky [a, *], Alexander V. Khoperskov [a], Alexander G. Losev [a]

[a] Volgograd State University, Russian Federation

Abstract

The goal of this study was to conduct the computing experiments on the use of the spatial temperature distribution and heat flow in biological tissues obtained on the basis of microwave radiometry, and to develop the predictive algorithm of their specific properties and conditions.

In the first stage, the data about the surface and deep temperature in different parts of the mammary glands of healthy women were used to build the model of heat flow in this body, proved that there is a lateral heat transfer from one part to another. Accounting for this phenomenon in the analysis of the spatial distribution of temperature in the breast with verified malignant tumours with installed localization made it possible to prove a several decision rules with a potentially high diagnostic efficiency.

Based on the assumption about spatial variation of the dielectric constant and electrical conductivity in biological tissue at the installation site and subsequent remodeling of tissue-engineered constructs to develop in similar patterns, and to be capable of the same impact on brightness temperature of the tissues under the antenna of a microwave radiometer, we conducted simulation in the second phase of the study. The crucial equations, being able to differentiate different states of adaptation (remodeling) of tissue-engineered constructs were offered, that can be used in tissue engineering as creating data structures, also for monitoring postimplantation period.

Keywords: microwave thermography, spatial temperature distribution, thermal transfer, brightness temperature, mammary glands, breast cancer, tissue engineering constructs, mathematical modeling, thermal simulation.

1. Introduction

New approaches to the reconstruction of organs and tissues, which were lost or irreversibly damaged as a result of illness, based on the use of tissue-engineered constructs (TEC) and cellular technologies, described in aggregate as TERM (tissue engineering and regenerative medicine) technologies. Biomimetic and biocompatible properties are fundamental for these products. Their presence provides complete or partial replacement of implant material by proper own tissue without any inflammatory reactions within the projected time (Wang et al., 2014; Maitz, 2015). In other cases, as a result, only a dense integration between the implant and surrounding tissues seems to be a general task of implantation (Jang et al., 2011; Albertini et al., 2015).

* Corresponding author
E-mail addresses: shiroky.aa@volsu.ru (A.A. Shiroky)

The undoubted purpose of the innovation in the field of manufacturing a variety of TEC is to make a more accurate reproduction of the structural and functional characteristics for prosthetic tissue. However, most studies usually focus on the structural biomimetics, which implied the restoration of the required functional characteristics after remodeling TEC in native host tissue (O'Brien, 2011; Park et al., 2016). This explains the comparative scarcity of works devoted to the analysis of the recovery of the functional status of an implantation region in the dynamics (Lu et al., 2013; Hwang et al., 2015). Typically, this analysis is carried out using specially designed options, which were not directly determined by real biochemical and physiological processes in the place of TEC installation (Guliak et al., 2014).

Research of heat transfer in system 'TEC – the surrounding tissue' due to remodeling is strongly important to explain these processes from the standpoint of the biochemistry and physiology of regeneration. First, the TEC remodeling is the phase process, which key points established as cell seeding, growth of blood vessels, resorption of the scaffold matter, and the synthesis of new extracellular matrix (Fitzpatrick, 2015; Mao, 2015). All of these components are differently connected to the heat input in the system and to own heat production in it. Second, the change of physico-chemical properties of the scaffold matter, as its transition in the host extracellular matrix, affects the characteristics of thermal conductivity, which is complicated by the spatial heterogeneity of tissues.

In this paper we analyze the possibility to simulate three-dimensional heat transfer, determine the spatial distribution of temperatures in the system 'TEC – the surrounding tissue', and build predictive algorithms for tissues, containing TEC at different stages of remodeling in host one. This approach is constructed by analogy with the cases for tissues with volume pathological focuses based on spatial heterogeneity of thermal distribution in tissues (Khoperskov et al., 2014; Losev et al., 2015).

2. Material and Methods

2.1. The measuring the spatial temperature distribution of in biological tissues

As a dataset, in the first phase of the study we used the results of measurements of surface and deep temperatures in different breast areas by microwave radiometry (MWR) is combined with surface infrared thermometry. This method is an important tool for breast cancer diagnosis, although it has a low enough nosological specificity (Leroy et al., 1998; Wurst et al., 2006; Kelly et al., 2011). Both most dangerous fast-growing tumors, and cases of marked proliferation, mastopathy, or inflammatory processes in mammary gland may be included in 'red group' after cohort survey (Kelly et al. 2012). To increase the sensitivity and specificity of this method, the spatial heterogeneity of the temperature distribution, their variances, or mirror asymmetry may be realized in several automated algorithms (Bardati, 2008; Vesnin et al., 2008; Shin et al., 2013).

We choose application MWR-method (Filatov et al., 2013), which allowed a direct contact between antenna and human body during the measurement. The technique was realized using radiometer RTM-01-RES Imaging system (RES Ltd., Russia). At frequencies of 1.1–1.6 GHz MWR demonstrated sufficient sensitivity to distinguish clinically significant temperature changes in tissues up to 4 cm depth in biological tissue (Umadevi et al., 2011). Modeling the thermal and electromagnetic processes in kidneys and brain showed a good agreement with the experimental MWR results (Gouzouasis et al., 2010; Stauffer et al., 2014). The use of this method for early diagnosis of vascular diseases such as atherosclerosis and varicose veins of the lower extremities, have received encouraging professional responses (Toutouzas et al., 2012; Stavrov et al., 2013).

The control sample included the results of measurements in healthy women 20-48 years without any breast pathology on clinical examination. The following exclusion criteria were established: any information about breast pathology in anamnesis (1), pregnancy (2), lactation (3), inner genital pathology (4), hormonal disorders (5), chronic infectious diseases or acute infections of less than 1 month before the survey (6), insufficiency of blood circulation (7). In the end, the sample included the results of an examination of 31 women. All calculations were carried out separately for the right and left mammary glands, given the presence of a physiological bilateral asymmetry (Vesnin et al., 2008).

The main sample included MWR data of the 78 women of the same age range, which had clinically proven breast cancer in the form of three-dimensional focus of accurate localization. Primary-dissociated, neglected, and doubtful cases were excluded from this sample.

Quantitative data were processed using Statistica 8.0 (StatSoft Inc., USA). Results were shown as Median [1st quartile ÷ 3rd quartile]. To prove the validity of differences for multiple groups the non-parametric ANOVA criterion was used; P values < 0.05 were considered statistically significant.

2.2. Modeling the heat transfer

Numerical simulation of electromagnetic radiation of tissues, including tumors, was based on the equations of heat conduction and Maxwell in the stationary approximation (Vesnin et al., 2010):

$$\vec{\nabla}\{k(x,y,z)\vec{\nabla}T(x,y,z)\} = -Q_{bl}(x,y,z) - Q_{met}(x,y,z), \quad (1)$$

$$\nabla^2\vec{E}(x,y,z) + \omega_0\mu_0\varepsilon_0\varepsilon(x,y,z)\vec{E}(x,y,z) = 0 \quad (2)$$

where k is the thermal conductivity coefficient; T – temperature; Q_{bl} – heat input with blood flow (determined by the balance of the arterial Q_a and venous Q_v heat transfer); Q_{met} is the heat source connected to metabolic processes in tissues (Fig. 1); $\vec{E}$ – vector of the electric field; ε – dielectric permittivity; ∇ is the nabla operator, and ω_0 is the radiation frequency.

Heat transfer from biological tissue to air at the interface, specified unit normal to the surface vector, defined by the condition:

$$\left(\vec{n},\vec{\nabla}T\right) = \frac{h_{air}}{k(x,y,z)}\left(T(x,y,z) - T_{air}\right). \quad (3)$$

Complex geometries and multi-component structure by using the methods of finite-difference approximations of the differential equations requires special numerical unstructured grids (Ng, 2004; Lin et al., 2009) and tasks of the boundary conditions (3) on a complex surface. The use of tetrahedra as elements of the grid is convenient for the simulation of radiation propagation in biotissue (Seteikin et al., 2010).

Fig. 1 shows the scheme of heat exchange between the biological tissues and the environment with the temperature T_{air}. It significantly depends on the heat transfer coefficient h_{air}, which can be taken equal to $h_{air} \approx 13.5$ W/(m·°C) for our case. A strong spatial heterogeneity of physical parameters is the distinctive feature of these biological tissues (Losev et al., 2015).

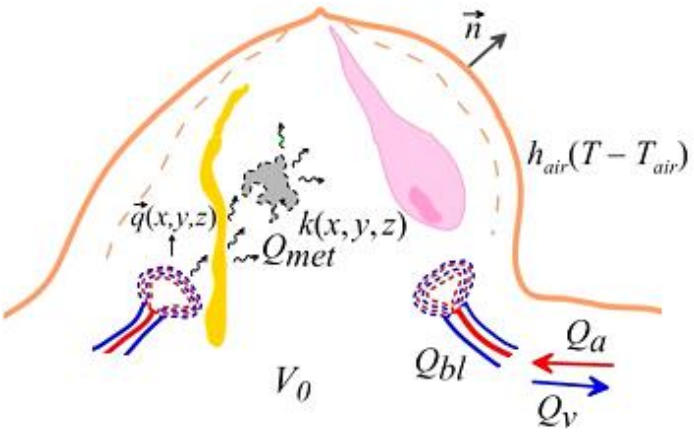

Fig. 1. The heat input Q_{bl}, own heat generation Q_{met}, heat exchange with air, and the internal heterogeneity of the structure are the fundamental processes characterizing the spatial features of heat transfer in the volume of breast tissue V_0. Explanations are following in the text.

Coefficient of thermal conductivity of tissues varies in the range of 0.15–0.7 W/(m·°C). The most important factor is the specific water content due to the strong dependence of tissue density, heat capacity and thermal conductivity from the value of this indicator (Table 1).

The presence of a malignant tumor to the greatest extent modifies the distribution of the specific heat generation $Q_{met} \approx 250\text{-}70000$ W/m^3 and flow parameters.

Table 1. The main physical characteristics of biological tissues, necessary to calculate the volumetric heat transfer in the body, generally at (Herman I.P., 2007; Afrin et al., 2011; Li et al., 2014)

Human tissues	Density, g/sm^3	Heat capacity, J/(g·°C)	Termal conductivity, W/(m·°C)
Skin	1.10 – 1.50	2.93 – 3.45	0.45 – 0.50
Blood	1.05 – 1.06	3.60 – 3.90	0.53 – 0.55
Adipose tissue	0.85 – 0.92	2.25 – 2.30	0.20
Connective tissue and muscles	1.04 – 1.10	3.30 – 3.36	0.50
Human body in common	1.04	3.35	0.48

Features of use of these general formulas and its approximation to specific calculations in the case of heat transfer in the tissues with the pathological focus or the TEC, following if result statement.

3. Results

3.1. Spatial temperature distribution in mammary glands

Table 2 shows the sample characteristics for control group of healthy women. Since the distribution in the samples is not parameterized, the median characteristics in quartiles 1 – 3 were presented.

The dispersion of inside temperatures at the measuring points 0 – 8 are in the range from 0.14 (point 0) to 0.37 (point 2). One way ANOVA shows that the sample with 95% probability does not differ. However, sampling of measurement results in point 9 (axillary region) has significant differences from the results in the breast.

In the case of surface temperature differences are brighter. The dispersion values are from 0.39 (measuring point 1) to 0.95 (point 0), which was probably due to differences in external conditions in examination procedure. U-test (Mann-Whitney) for the measurement data in pairs of adjacent points revealed no differences, although the ANOVA test showed that the alternative hypothesis was true. In a similar way the difference of external and internal temperatures manifested themselves.

Table 2. Spatial distribution and gradient of temperature in intact mammary glands of practically healthy women (Me [Q1 ÷ Q3])

Points	Surface temperature ˚C	Inner temperature ˚C	Temperature gradients
Left breast			
0 (Mamilla)	32.8 [32.6 ÷ 33.7]	34.5 [34.3 ÷ 34.8]	1.5 [1.0 ÷ 2.1]
1	32.9 [32.7 ÷ 33.3]	34.6 [34.1 ÷ 35.0]	1.6 [1.2 ÷ 2.1]
2	33.2 [32.7 ÷ 33.7]	34.6 [34.2 ÷ 34.9]	1.5 [1.0 ÷ 1.9]
3	33.4 [32.6 ÷ 33.8]	34.7 [34.3 ÷ 34.9]	1.2 [0.8 ÷ 2.1]
4	33.2 [32.7 ÷ 33.5]	34.4 [34.2 ÷ 34.8]	1.3 [1.0 ÷ 1.7]
5	32.9 [32.1 ÷ 33.3]	34.4 [34.1 ÷ 34.7]	1.7 [1.1 ÷ 2.3]
6	32.5 [31.9 ÷ 33.1]	34.3 [33.9 ÷ 34.7]	2.0 [1.5 ÷ 2.4]
7	32.5 [32.2 ÷ 33.0]	34.4 [34.0 ÷ 34.8]	1.9 [1.5 ÷ 2.3]

8	33.0 [32.4 ÷ 33.4]	34.5 [34.2 ÷ 35.0]	1.7 [1.2 ÷ 2.1]
9 (Axillary)	33.1 [32.7 ÷ 33.5]	34.9 [34.4 ÷ 35.3]	1.8 [1.4 ÷ 2.2]
Right breast			
0 (Mamilla)	32.7 [32.2 ÷ 33.2]	34.5 [34.1 ÷ 35.0]	1.6 [1.2 ÷ 2.4]
1	33.1 [32.8 ÷ 33.6]	34.6 [34.1 ÷ 35.0]	1.3 [0.8 ÷ 2.1]
2	32.9 [32.2 ÷ 33.6]	34.5 [34.2 ÷ 34.8]	1.6 [1.1 ÷ 2.2]
3	32.7 [32.1 ÷ 33.3]	34.3 [34.1 ÷ 34.7]	1.6 [1.0 ÷ 2.2]
4	33.1 [32.4 ÷ 33.7]	34.5 [34.1 ÷ 34.7]	1.4 [0.9 ÷ 2.0]
5	33.0 [32.4 ÷ 33.4]	34.3 [34.1 ÷ 34.6]	1.5 [1.1 ÷ 1.9]
6	32.4 [31.8 ÷ 33.1]	34.2 [33.8 ÷ 34.6]	1.8 [1.4 ÷ 2.4]
7	32.7 [32.2 ÷ 33.0]	34.4 [34.1 ÷ 34.6]	1.7 [1.5 ÷ 2.1]
8	32.8 [32.6 ÷ 33.2]	34.5 [34.0 ÷ 35.0]	1.5 [1.2 ÷ 2.0]
9 (Axillary)	33.1 [32.6 ÷ 33.6]	35.0 [35.3 ÷ 35.3]	1.7 [1.3 ÷ 2.1]

Statistically insignificant differences of inner temperatures in healthy women related to the fact that the heat input to the breast came from the evenly heated chest muscles and also the blood close to the temperature, while the foci of abnormally high metabolic activity of cells (with a corresponding increase in temperature) do not exist in its tissue.

Fig. 2 shows that a relatively uniform distribution of inner temperatures, at the surface we can see a fairly large range of temperatures, which corresponded to the fluctuations of the vertical temperature gradient from 1.2 to 2.0 °C.

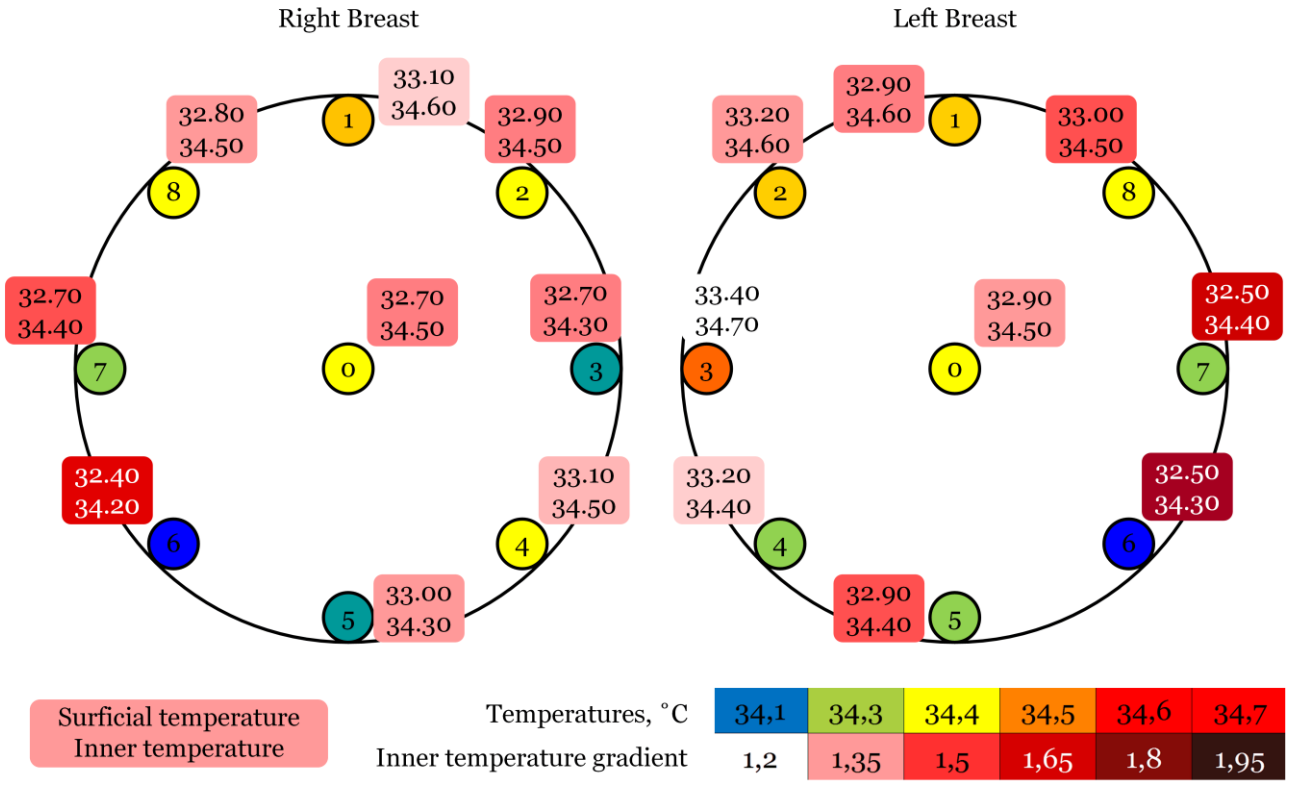

Fig. 2. The spatial distribution of temperatures (°C) inside the right and left breasts of healthy women based on the MWR results. Numbers '0-9' represent the point of withdrawal of surface and inner temperatures according to the methodology of the breast survey (Vesnin et al., 2008).

One of important feature of method used to measure the internal temperatures, is that the average temperature of the tissues inside the cylinders with a depth of 5-7 cm and a diameter equal to the diameter of the applicator antenna became an index for measurement. The surface temperature measured by contact method using combined sensor – that is, the measurements were carried out exactly on the axis of the cylinder. With this approach, increased spread of surface temperatures in the breast can be explained only by redistribution (lateral transfer) of heat inside the body, between the cylinders of the measurement.

3.2. The calculation of the lateral thermal transfer in normal mammary glands

Thermal radiation of biotissue consists of heat introduced with the blood flow, and also of metabolic energy. The value of the latter in breast is ten times smaller in absolute value, and the difference between arterial and venous temperature is almost exclusively a reflection of the magnitude of heat transfer from the surface of the body (Rodrigues et al., 2013). In this regard, the contributions of the metabolic processes (Q_{met}) to the spatial distribution of heat transfer in unchanged mammary gland, are comparable to the measurement error, and therefore they will continue to be excluded from consideration.

Thus, breast without the pathological focus primarily receives heat from the blood flow, and lose it through heat output to the environment. Since the quantity of blood in the tissue under physiological conditions, is equal to the quantity leaving the body all the difference in stored thermal energy to be dissipated into the environment through the skin. From these positions, the points of the breast with the greatest difference of deep and surface temperatures correspond to the zones with the most intensive heat transfer to the environment.

The radiometer measures the average temperature in the cylinder with a diameter of about 5 cm and depth of 5-7 cm. This corresponds to a volume of tissue greater than 450 cm^3. In this connection within the space, measured in the projection of any point MWR, quite correct to highlight in the breast the conditional cylinder from the pectoral muscle to the skin a mass of 100 g. Totality of these nine volumes was adopted for building the spatial model.

To calculate the volume of the spatial heat transfer in the mammary gland, we use the fact that, according to adopted minimize the Q_{met} contribution and approximate process to stationary state in time that is commensurate with the measurement period, all surplus energy from the inner core of the body is equal to the energy transfer to the skin. It, in turn, is equal to the amount of heat transfer into the surrounding tissue.

Calculations it is more convenient to start from the transfer of energy inside the breast. The total amount of heat given to the conventional cylinder Q_i (J) we find by the formula:

$$Q_i = m \cdot C \cdot \Delta T / t_{cap}\ , \quad (6)$$

where m is the mass of the conditional cylinder of tissue, g; C – thermal conductivity, J/(g·°C); ΔT – the difference of surface and inner temperatures, °C; t_{cap} – average time of capillary blood flow, numerically equal to the duration of one cycle of heat transfer, c.

Since the average specific heat of tissue is 3.35 J/(g·°C), and the average time of capillary blood flow t_{cap} is approximately 30 seconds, the total quantity of heat given to the conventional cylinder weight of 100 g per unit time, will be $Q_i(\Delta T) = 3.35 \cdot 100 \cdot \frac{\Delta T}{30} = 11.17\Delta T$, J.

Fig. 3 demonstrates a vertical flow of heat energy after their calculation in the literal expression. It is clearly seen that the system has both areas with very moderate heat transfer from the deep tissues to the skin, and a relatively large ones, with fluctuations of values from 14.5 to 21.2 J. A similar pattern can be partially explained by the spatial heterogeneity of small-scale structure of mammary gland, and of course, it influences the interstitial heat transfer processes in this organ.

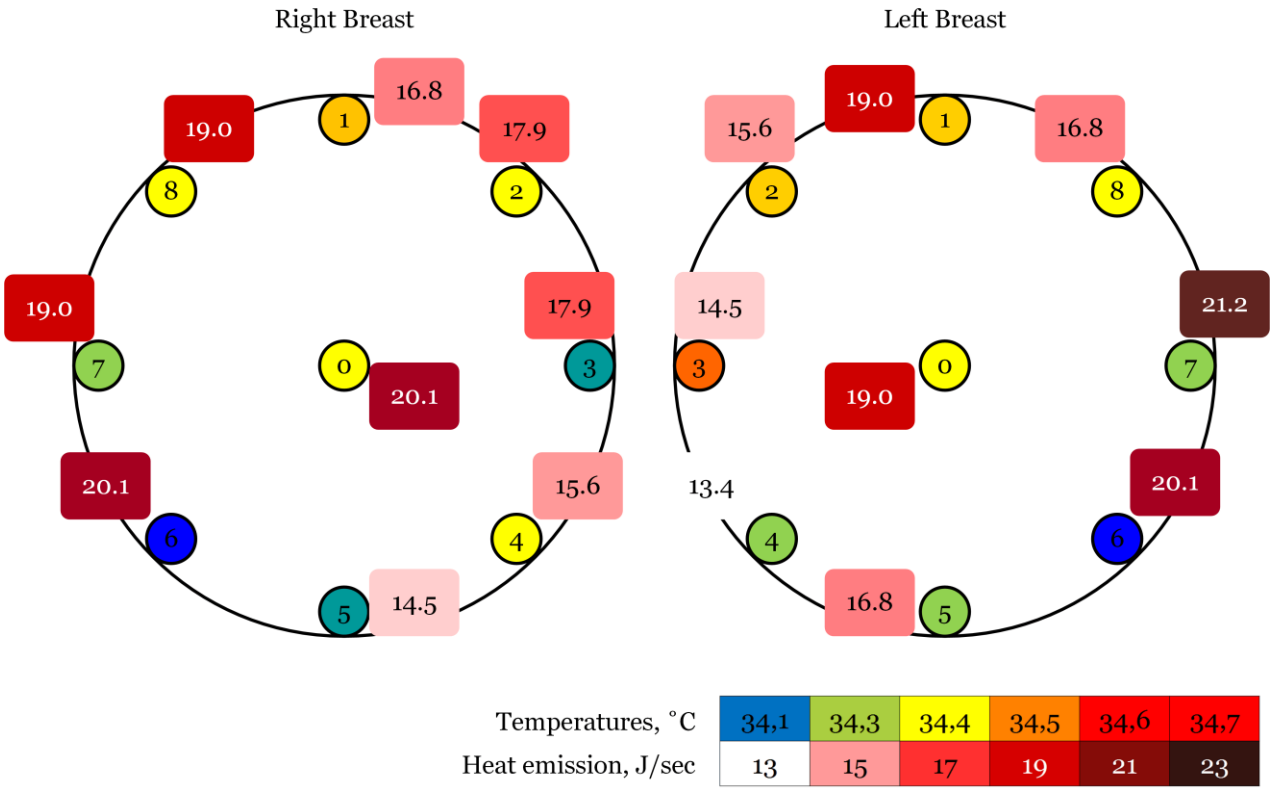

Fig. 3. Heat transfer (J) moved every second from the depths to the surface in the conventional areas in the right and left breast mass of 100 g in the projection points of the MWR.

Assume that the breast can be divided into nine non-overlapping segments corresponding to cylinders with axes perpendicular to the skin surface and passing through the point of measurement 0 – 8. Assume also that the mass of the tissues inside these segments is equal to 100 grams.

Then, knowing the difference between external and internal temperatures in the cylinders of measurement, it is possible to obtain the total amount of heat dissipated into the environment: $Q = \sum_i Q_i$. Since the process is stationary, then the quantity of heat flowing into the breast is also equal to Q.

Let us now consider the heat transfer inside the cylinder. Most of the energy passes along the cylinder from the depths to the surface of body. Constantly there is an exchange of energy between adjacent cylinders. Since both inner and surface temperatures of the cylinders are different, the amount of heat, adopted and diffused by them will also be different. We calculate them as follows:

$$Q_i^{in} = \frac{1}{9}Q + Q_i\left(T_{mean}^{in} - T_i^{in}\right)$$

$$Q_i^{out} = \frac{1}{9}Q + Q_i\left(T_{mean}^{sf} - T_i^{sf}\right) \text{ или } Q_i^{out} = \frac{1}{9}Q - Q_i\left(T_{mean}^{sf} - T_i^{sf}\right),$$

where T_i^{in}, T_i^{sf} is, respectively, inner and surface temperature of the ith cylinder, $T_{mean}^{in}, T_{mean}^{sf}$ – average temperatures in the cylinders 0 – 8.

Here is an example of calculated data for right breast of the healthy woman 36 years old (Table 3).

Table 3. Evaluation data of heat transfer between measurement cylinders for one case (healthy woman, 36 years)

	0	1	2	3	4	5	6	7	8	Mean
Inner temperature ˚C	35.2	34.6	35.2	34.7	34.6	35	34.6	34.5	34.5	34.8
Surface temperature ˚C	32.9	32.8	33.6	32.7	32.4	33.1	32.3	32.1	32.5	32.7
Inner temperature gradient	2.3	1.8	1.6	2.0	2.2	1.9	2.3	2.4	2.0	—
Heat emission of cylinder, J/sec	25.7	20.1	17.9	22.3	24.6	21.2	25.7	26.8	22.3	23.0
Evaluated cylinder heat income, J/sec	27.8	21.1	27.8	22.2	21.1	25.6	21.1	20.0	20.0	—
Evaluated cylinder heat outcome, J/sec	25.1	24.0	32.9	22.8	19.5	27.3	18.4	16.1	20.6	—
Heat excess, J/sec	2.7	-2.9	-5.1	-0.6	1.6	-1.7	2.7	3.8	-0.6	—
Average cylinder temperature, ˚C	34.1	33.7	34.4	33.7	33.5	34.1	33.5	33.3	33.5	—

Fig. 4 shows the main directions of heat transfer in the breast of this woman. Note that the average temperature of the cylinder 2 is the highest. Temperature points {0, 5}, {1, 3}, and {4, 6, 7, 8} are within the error of the measuring instrument RTM-01-RES. The direction of possible lateral heat transfer is oriented from the outer portions of the breast (the cylinders corresponding to points 6 and 7 during the MWT) to the upper-medial quadrant (point 2).

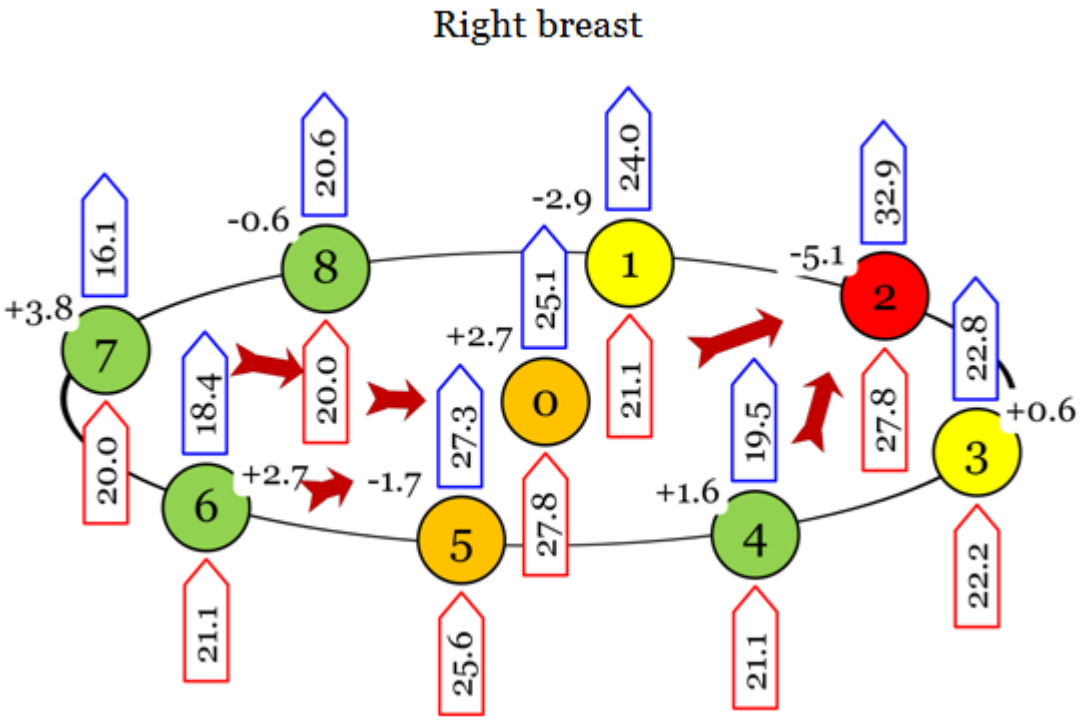

Fig. 4. Probable heat transfer routes in right breast for one case (healthy female, 36 years).

The calculation of the actual values of heat transfer will require, apparently, three-dimensional models to build which is necessary to make a series of additional measurements. Therefore, this aspect remains beyond the scope of this article.

3.3. Calculation of heat transfer in the presence of the pathological focus

Table 3 presents the following statistics on the temperature in the healthy breast and breast with the diagnosed cancers: the inner temperature of the hottest point given to internal axillary temperature (1); the inner temperature of a point on the opposite side of the body (2); the temperature difference between the hottest point and its opposite (3).

Table 4. Spatial distribution and temperature gradients in the mammary glands in the presence of malignant tumors of the installed localization (Me [Q1 ÷ Q3])

Breast	Healthy women	Breast cancer
Left breast		
Most hot point temperature, ˚C	34.9 [34.7 ÷ 35.2]	35.2 [34.6 ÷ 35.9]
Opposite point temperature, ˚C	34.5 [34.0 ÷ 34.8]	34.5 [33.6 ÷ 35.2]
Temperature difference between axillary and most hot point, ˚C	–0.1 [–0.4 ÷ 0.1]	0.1 [–0.4 ÷ 0.6]
Temperature difference between axillary and opposite point, ˚C	0.4 [–0.2 ÷ 0.8]	0.8 [0.4 ÷ 1.4]
Most hot point and its opposite difference, ˚C	0.4 [0.1 ÷ 1.0]	0.7 [0.4 ÷ 1.1]
Right breast		
Most hot point temperature, ˚C	35.05 [34.2 ÷ 35.7]	35.1 [34.2 ÷ 35.7]
Opposite point temperature, ˚C	34.4 [34.0 ÷ 34.9]	34.3 [33.5 ÷ 35.0]
Temperature difference between axillary and most hot point, ˚C	0.1 [–0.3 ÷ 0.3]	0.2 [–0.2 ÷ 0.5]
Temperature difference between axillary and opposite point, ˚C	0.4 [0.1 ÷ 0.9]	1.1 [0.5 ÷ 1.4]
Most hot point and its opposite difference, ˚C	0.6 [0.1 ÷ 0.8]	0.8 [0.4 ÷ 1.2]

Analysis of variance revealed no significant differences between samples. The temperature distribution was largely dependent on the individual structure of the body; any regularities between the structure of the gland and the area of disease were also not installed. However, it is quite obvious that the additional source of heat may change the structure of the heat transfer inside the body.

Here is an example of calculated data for the right breast women 38 years with diagnosed cancer focus (Table 5).

Table 5. Evaluation data of heat transfer between measurement cylinders for one case (woman with breast cancer, 38 years)

	0	1	2	3	4	5	6	7	8	Mean
Inner temperature ˚C	34.3	34.5	34.8	34.4	34.1	34.7	34.7	35	34.4	34.5
Surface temperature ˚C	33	32.9	33.2	32.8	32.8	33	32.9	33.8	33	33.0
Inner temperature gradient	1.3	1.6	1.6	1.6	1.3	1.7	1.8	1.2	1.4	—
Heat emission of cylinder, J/sec	14.5	17.9	17.9	17.9	14.5	19.0	20.1	13.4	15.6	16.8
Evaluated cylinder heat income, J/sec	14.0	16.3	19.6	15.1	11.8	18.5	18.5	21.8	15.1	—
Evaluated cylinder heat outcome, J/sec	16.3	15.1	18.5	14.0	14.0	16.3	15.1	25.2	16.3	—
Heat excess, J/sec	-2.2	1.1	1.1	1.1	-2.2	2.2	3.4	-3.4	-1.1	—
Average cylinder temperature, ˚C	33.7	33.7	34.0	33.6	33.5	33.9	33.8	34.4	33.7	—

Note that the average temperature of the cylinders 7 and 2 is the highest. Cylinders {0, 1, 5, 6, 8} are somewhat colder, and the temperature in the MWR points {3, 4} markedly (by about half a degree) is below.

Fig. 5 shows that the direction of possible lateral transfer in the same way as in the case with a healthy body, directed from the cylinders corresponding to points 5 and 6 at MWR. But now the lateral heat transfer occurs in two quadrants – lower-medial (point 2) and the left one, where the pathology was focused (point 7). Note that the average temperature of the cylinders 7 and 2 is the highest. Cylinders {0, 1, 5, 6, 8} are somewhat colder, and the temperature in the MWR points {3, 4} is markedly (by about half a degree) below.

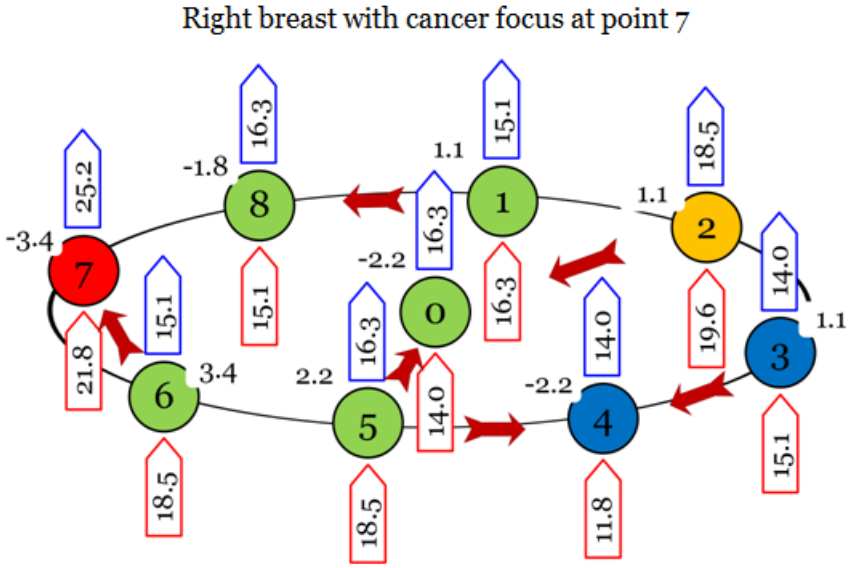

Fig. 5. Probable heat transfer routes in right breast for one case (woman with breast cancer, 38 years).

3.4. Transformation models for the case with TEC presence

Let us consider the use of such building for the analysis of heat transfer in tissue containing TEC. If the scaffold has a cylindrical shape, covering the soft tissue defects with a fairly uniform distribution of properties, only three positions can be vary in its properties: the soft tissues outside of the scaffold (point 0), the border 'soft tissue – scaffold' (point 1), and its geometric center (point 2).

As the remodeling, the ratio of the individual components (substances scaffold, blood vessels and host tissues), in points 1 and 2 will change. To calculate the heat capacity and thermal

conductivity of the newly formed tissue, we used the ratio of the components obtained in the experimental study, where scaffolds based on natural polymers chitosan and polycaprolactone have been successfully installed (Novochadov et al., 2013; Ivanov et al., 2015; Modulevsky et al., 2016); the basic design characteristics are given in Table 5. From these data it is clearly seen that as scaffold remodeling is accompanied by decrement of heat capacity, while the conductivity increased.

Table 5. The design physical characteristics of biological tissue due to scaffold remodeling

	Surrounding soft tissues (point 0)	Time of remodeling	The TEC edge (point 1)	The TEC centre (point 2)
TEC, %	0	Installation 4 week 12 week	100 67 0	100 88 9
Vessels, %	5	Installation 4 week 12 week	0 9 7	0 3 6
Soft tissues, %	95	Installation 4 week 12 week	0 24 93	0 10 85
The estimated heat capacity, J/(g·°C)	3.35	Installation 4 week 12 week	3.85 3.72 3.34	3.85 3.83 3.37
The estimated termal conductivity, W/(m·°C)	0.50	Installation 4 week 12 week	0.35 0.40 0.50	0.35 0.37 0.46

Fig. 5 shows the calculated values of the relevant thermal transfers, which direction, to the extent of scaffold remodeling, have been reversed.

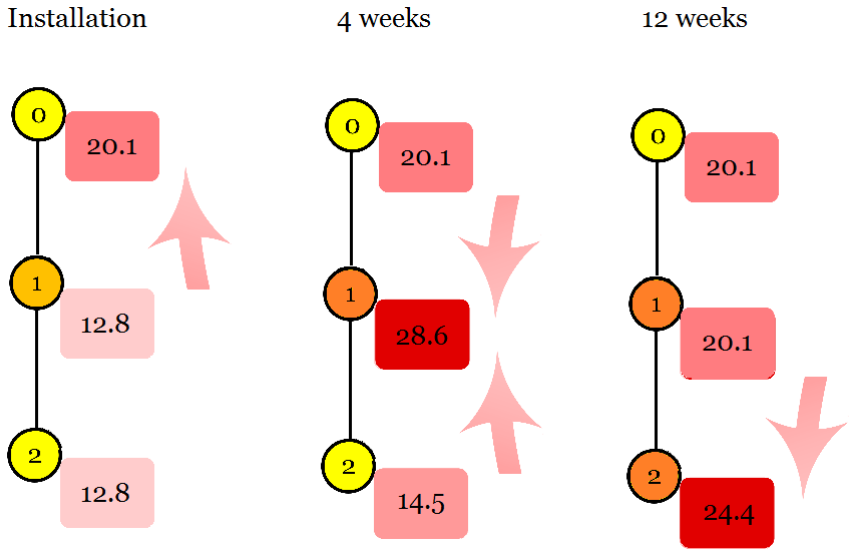

Fig. 5. The amount of energy (J) that is moved every second of the depths to the surface in the field of installation of tissue-engineered cylindrical constructs (diameter 5 cm; height 0.5 cm) as replacement of its material by host tissues. Number '0' shows point in the surrounding tissue; number '1' is the point at the border of the structure and surrounding tissue; number 2 shows the place in the center of the TEC. Arrows indicate the path of lateral heat transfer.

The revealed regularities can be considered as in tissue engineering when setting properties of the newly developed structures (Gu et al., 2016; Li et al., 2016), and for monitoring postimplantation period where it could obtain a non-invasive way information about the most likely mechanobiology properties of the implanted object in the dynamics of its remodeling (Giorgi et al., 2016).

4. Conclusion

This study demonstrates the presence of lateral heat transfer from one part of the breast to other ones and the ability to determine its most probable vectors in the real bodies of healthy women and cases with presence of malignant neoplasms. It was shown the identification and calculation of such heat flow vectors had independent diagnostic potential.

The algorithm of calculations for tissue with pathological focus, with minor modifications, is applicable for analyzing heat transfer in tissue containing TEC. Calculations of heat transfer for such systems in different periods after the TEC installation demonstrate the presence of a lateral heat transfer, and as scaffold remodeling in the host tissue the direction of heat transfer changes from a predominantly centrifugal to centripetal. This transition is well marked and can be used for non-invasive monitoring of adaptation in the postimplantation period.

5. Acknowledgements

The study was carried out with financial support of Russian Foundation for Basic Research in the framework of a research projects No. 15–47–02475–Povolzhie and No. 15–47–02642–Povolzhie.

References

Afrin et al., 2011 – *Afrin N., Zhang Y., Chen J.K.* (2011). Thermal lagging in living biological tissue based on nonequilibrium heat transfer between tissue, arterial and venous bloodsInternational. *J. Heat Mass Transfer.* 54(11–12), 2419–2426. doi: 10.1016/j. ijheatmasstransfer. 2011.02.020

Albertini et al., 2015 – *Albertini M., Fernandez-Yague M., Lázaro P., et al.* (2015). Advances in surfaces and osseointegration in implantology. Biomimetic surfaces. *Med. Oral Patol. Oral Cir. Bucal.* 20(3), e316–e325. doi: 10.4317/medoral.20353.

Bardati, 2008 – *Bardati F., Iudicello S.* (2008). Modeling the visibility of breast malignancy by a microwave radiometer. *IEEE Trans. Biomed. Eng.* 55(1), 214-221. doi: 10.1109/TBME.2007.899354

Filatov et al., 2013 – *Filatov A.V., Ubaichin A.V., Bombizov A.A.* (2013). A two-receiver microwave radiometer with high transfer characteristic linearity. *Measurement Techniques.* 55(11), pp. 1281–1286. doi: 10.1007/s11018-013-0121-5

Fitzpatrick, 2015 – *Fitzpatrick L.E., McDevitt T.C.* (2015). Cell-derived matrices for tissue engineering and regenerative medicine applications. *Biomater. Sci.* 3(1), 12–24. doi: 10.1039/C4BM00246F

Giorgi et al., 2016 – *Giorgi M., Verbruggen S.W., Lacroix D.* (2016). In silico bone mechanobiology: modeling a multifaceted biological system. *Wiley Interdiscip. Rev. Syst. Biol. Med.* 8(6), 485–505. doi: 10.1002/wsbm.1356

Gouzouasis et al., 2010 – *Gouzouasis I.A., Karathanasis K.T., Karanasiou I.S., Uzunoglu N.K.* (2010). Contactless passive diagnosis for brain intracranial applications: a study using dielectric matching materials. *Bioelectromagnetics.* 31(5), 335–349. doi: 10.1002/bem.20572

Gu et al., 2016 – *Gu B.K., Choi D.J., Park S.J., et al.* (2016). 3-Dimensional bioprinting for tissue engineering applications. *Biomater Res.* 20: 12. doi: 10.1186/s40824-016-0058-2

Guliak et al., 2014 – *Guilak F., Butler D.L., Goldstein S.A., Baaijens F.P.T.* (2014). Biomechanics and mechanobiology in functional tissue engineering. *J. Biomech.* 47(9): 1933–1940. doi: 10.1016/j.jbiomech.2014.04.019

Herman I.P., 2007 – *Herman I.P.* (2007). Physics of the Human Body. Berlin; Heidelberg: Springer-Verlag, 880 p.

Hwang et al., 2015 – *Hwang J., Jeong Y., Park J.M., et al.* (2015). Biomimetics: forecasting the future of science, engineering, and medicine. *Int. J. Nanomedicine.* 10: 5701–5713. doi: 10.2147/IJN.S83642

Ivanov et al., 2015 – *Ivanov A.N., Kozadaev M.N., Bogomolova N.V., et al.* (2015). Biocompatibility of polycaprolactone and hydroxyapatite matrices in vivo. *Cell Tissue Biol.* 9(5), 422-429. doi:10.1134/S1990519X15050077

Jang et al., 2011 – *Jang H.W., Kang J.K., Lee K., et al.* (2011). A retrospective study on related factors affecting the survival rate of dental implants. *J. Adv. Prosthodont.* 3(4), 204-215. doi: 10.4047/jap.2011.3.4.204

Kelly et al., 2011 – *Kelly P., Sobers T., Peter B.S., et al.* (2011). Temperature anomaly detection and estimation using microwave radiometry and anatomical information. *Proc. SPIE.* e79614. doi: 10.1117/12.878136

Kelly et al., 2012 – *Kelly, P. Sobers T., Peter B. S. et al.* (2012). Microwave radiometric signatures of temperature anomalies in tissue. *Proc. SPIE 2012.* e831368. doi: 10.1117/12.910785.

Khoperskov et al., 2014 – *Khoperskov A.V., Khrapov S.S., Novochadov V.V., Burnos D.V.* (2014). The effect of small-scale mammary glands structure on the distribution of the deep temperature using the microwave radiometry diagnostics. *J. Volgograd State Univ. 1: Mathematics. Physics.* 5 (25), 60-68. [in Rus., Eng. abstr.]

Leroy et al., 1998 – *Leroy Y., Bocquet B., Mammouni A.* (1998). Non-invasive microwave radiometry thermometry. *Physiol. Means.* 19, 127-148.

Li et al., 2014 – *Li L., Liang M., Yu B., Yang S.* (2014). Analysis of thermal conductivity in living biological tissue with vascular network and convection. *Int. J. Thermal Sci.* 86, 219–226. doi: 10.1016/j.ijthermalsci.2014.07.006

Li et al., 2016 – *Li J., Chen M., Fan X., Zhou H.* (2016). Recent advances in bioprinting techniques: approaches, applications and future prospects. *J. Transl. Med.* 14, e271. doi: 10.1186/s12967-016-1028-0

Lin et al., 2009 – *Lin Q.Y., Yang H.Q., Xie S.S., et al.* (2009) Detecting early breast tumour by finite element thermal analysis. *J. Med. Eng. Technol.* 33(4), 274-280. doi: 10.1080/03091900802106638

Losev et al., 2015 – *Losev A.G., Khoperskov A.V., Astakhov A.S., Suleymanova Kh.M.* (2015). Problems of measurement and modeling of thermal and radiation fields in biological tissues: analysis of microwave thermometry data. *J. Volgograd State Univ. 1: Mathematics. Physics.* 6 (31), 31-71. [in Rus., Eng. abstr.] doi: 10.15688/jvolsu1.2015.6.3

Lu et al., 2013 – *Lu T., Li Y., Chen T.* (2013). Techniques for fabrication and construction of three-dimensional scaffolds for tissue engineering. *Int. J. Nanomedicine.* 8, 337–350. doi: 10.2147/IJN.S38635

Maitz, 2015 – *Maitz M.F.* (2015) Applications of synthetic polymers in clinical medicine. *Biosurf. Biotribol.* 1(3), 161–176.

Mao, 2015 – *Mao A.S., Mooney D.J.* (2015). Regenerative medicine: Current therapies and future directions. *Proc. Natl. Acad. Sci. U. S. A.* 112(47), 14452–14459. doi: 10.1016/ j.bsbt.2015.08.002

Modulevsky et al., 2016 – *Modulevsky D.J., Cuerrier C.M., Pelling A.E.* (2016). Biocompatibility of subcutaneously implanted plant-derived cellulose biomaterials. *PLoS One.* 11(6): e0157894. doi: 10.1371/journal.pone.0157894

Ng, Sudharsan, 2004 – *Ng E.Y.-K., Sudharsan N.M.* (2004). Computer simulation in conjunction with medical thermography as an adjunct tool for early detection of breast cancer. *BMC Cancer.* 4(17), e6. doi: 10.1186/1471-2407-4-17.

Novochadov et al., 2013 – *Novochadov V.V., Semenov P.S., Lyabin M.P.* (2013). [Innovative approaches to scaffold technology optimization based on chitosan, in tissue engineering of articular cartilage]. *J. Volgograd State Univ. 10: Innovations.* (2), pp. 135-143. [in Rus., Eng. abstr.]

O'Brien, 2011 – *O'Brien F.J.* (2011) Biomaterials and scaffolds for tissue engineering. *Mater. Today.* 14, 88–95. doi: 10.1016/S1369-7021(11)70058-X

Park et al. 2016 – *Park K.D., Wang X., Lee J.Y., et al.* (2016). Research trends in biomimetic medical materials for tissue engineering: commentary. *Biomater Res.* 20: 8. doi: 10.1186/s40824-016-0053-7

Rodrigues et al., 2013 – *Rodrigues D.B., Maccarinia P.F., Salahic S., et al.* (2013). Numerical 3D modeling of heat transfer in human tissues for microwave radiometry monitoring of brown fat metabolism *Proc. SPIE 2013.* e8584. doi: 10.1117/12.2004931.

Seteikin et al., 2010 – *Seteikin A.Yu., Krasnikov I.V., Pavlov M.S.* (2010). [3-Dimentional model of light propagation in biological tissues]. [J. Saint Petersburg University. 11: Medicine]. (3), 166–172. [in Rus.]

Shin et al., 2013 – *Shin S.-W., Kim K.-S., Lee J.-W., et al.* (2013). Implementing graphic user interface system for microwave radiometry data to utilize breast cancer diagnosis. Transact. Korean Inst. Electr. Eng. 62(6), 818–824.

Stavrov et al., 2013 – *Stavrov T.A., Bukina E.V., Losev A.G., Zamechnik T.V.* (2013). [Mathematical verification of early recurrence of the varicose disease after the endovascular laser obliteration of the great saphenous vein according to data of the radiothermometry]. *J. New Med. Technol. (Tula).* 20(2), 14–18. [in Rus., Eng. abstr.]

Stauffer et al., 2014 – *Stauffer P.R., Rodrigues D.B., Maccarini P.F.* (2014). Utility of microwave radiometry for diagnostic and therapeutic applications of non-invasive temperature monitoring. *IEEE BenMAS (Benjamin Franklin Symposium on Microwave and Antenna Sub-systems).* doi: 10.13140/2.1.3762.0487.

Toutouzas et al., 2012 – *Toutouzas K., Drakopoulou M., Siores E. et al.* (2012). In vivo measurement of plaque neovascularisation and thermal heterogeneity in intermediate lesions of human carotid arteries. *Heart.* 98, 1716-1721. doi: 10.1136/heartjnl- 2012-302507

Umadevi et al., 2011 – *Umadevi V., Raghavan S.V., Jaipurkar S.* (2011). Framework for estimating tumour parameters using thermal imaging. *Indian J. Med. Res.* 134(5), 725–731. doi: 10.4103/0971-5916.91012.

Vesnin et al., 2008 – *Vesnin S.G., Kaplan A.M., Avakyan R.S.* (2008). [Advanced microwave radiometry of the breast]. *Meditzinskiy Al'manakh [Med. Almanac].* (3), 82–87.

Vesnin et al., 2010 – *Vesnin S.G., Sedankin M.K.* (2010). [Mathematical modeling of own radiation of human tissues in the microwave range]. *Biomeditzinskaya Radioelektronika [Biomedical Radio Electronics].* (9), 33–43. [in Rus., Eng. abstr.]

Wang et al., 2014 – *Wang J., Lü D., Mao D., Long M.* (2014). Mechanomics: an emerging field between biology and biomechanics. *Protein Cell.* 5(7), 518–531. doi: 10.1007/s13238-014-0057-9

Wust et al., 2006 – *Wust P., Cho C. H., Hildebrandt B., Gellermann J.* (2006). Thermal monitoring: invasive, minimal-invasive and non-invasive approaches. *Int. J. Hyperthermia.* 22(3), 255–262. doi: 10.1080/02656730600661149